

The thickness of H I in galactic discs under MOND: theory and application to the Galaxy

F. J. Sánchez-Salcedo^{1*}, K. Saha^{2,3} and C. A. Narayan⁴

¹*Instituto de Astronomía, Universidad Nacional Autónoma de México, Apt. Postal 70 264, C.P. 04510, Mexico City, Mexico*

²*Department of Physics, Indian Institute of Science, Bangalore 560012, India*

³*Raman Research Institute, Bangalore 560080, India*

⁴*Astronomisches Institut, Ruhr-Universität Bochum, Universitätsstrasse 150, 44780 Bochum, Germany*

Accepted xxxx Month xx. Received xxxx Month xx; in original form 2007 July 20

ABSTRACT

The outskirts of galaxies are a very good laboratory for testing the nature of the gravitational field at low accelerations. By assuming that the neutral hydrogen gas is in hydrostatic equilibrium in the gravitational potential of the host galaxy, the observed flaring of the gas layer can be used to test modified gravities. For the first time we construct a simple framework to derive the scaleheight of the neutral hydrogen gas disc in the MOND scenario and apply this to the Milky Way. It is shown that using a constant gas velocity dispersion of $\sim 9 \text{ km s}^{-1}$, MOND is able to give a very good fit to the observed H I flaring beyond a galactocentric distance of 17 kpc up to the last measured point ($\sim 40 \text{ kpc}$). Between 10 and 16 kpc, however, the observed scaleheight is about 40% more than what MOND predicts for the standard interpolating function and 70% for the form suggested by Famaey & Binney. Given the uncertainties in the non-thermal pressure support by cosmic rays and magnetic fields, MOND seems to be a plausible alternative to dark matter in explaining the Milky Way flaring. Studying the flaring of extended H I discs in external edge-on galaxies may be a promising approach to assess the viability of MOND.

Key words: galaxies: haloes – galaxies: kinematics and dynamics – galaxies: structure – gravitation – Galaxy: disc

1 INTRODUCTION

The success of MODified Newtonian Dynamics (MOND) in reproducing the observed velocity rotation curves of spiral galaxies without dark matter haloes is amazing. Only in about 10% of the roughly 100 galaxies considered in the context of MOND does the predicted rotation curve differ significantly from that observed (e.g., Sanders & McGaugh 2002). Bekenstein (2004) has suggested a theory that leave a door open to embed MOND within a physically acceptable dynamical framework. However, other aspects of MOND in spiral and elliptical galaxies are yet to be investigated. It would be desirable to see if MOND is able to reproduce the full three-dimensional structure of galaxies (e.g., Kuijken & Gilmore 1987; Hernquist & Quinn 1987; Buote & Canizares 1994; McGaugh & de Blok 1998; Milgrom 2001; Stubbs & Garg 2005; Nipoti et al. 2007).

The flaring of the H I gas layers has been used to determine the flattenings of dark haloes for a few external galaxies because it is sensitive to the shape of the dark matter

halo (e.g., Olling 1996; Bica & Combes 1997). The alternative theories to dark matter may also have observable consequences on the vertical structure of galactic discs. For instance, studies of the flaring of the H I discs have been able to rule out the magnetic alternative to dark matter because the magnetic pressure would produce extraordinary thick discs (Cuddeford & Binney 1993; Sánchez-Salcedo & Reyes-Ruiz 2004). In modified gravities such as MOND, where the gravity comes mainly from the disc, the potential may be much flatter leading to far more thin discs (e.g., Sánchez-Salcedo & Lora 2005). In this paper we suggest the usage of the flaring of H I discs to test modified gravities.

The Milky Way is an attractive target to carry out self-consistent tests because of the excellent flaring data, large radial extend and rather well-known distribution of stars and gas. In the conventional Newtonian view, Kalberla (2003) and Kalberla et al. (2007) have found no easy way to match a standard *flattened dark halo* to the Galactic flaring data. They discuss the role of support by non-thermal pressures, non-axisymmetric mass distributions of dark and baryonic matter, spiral structures and so on, and conclude that, besides a massive round dark halo, a self-gravitating dark mat-

* E-mail: jsanchez@astroscu.unam.mx

ter disc with mass $\sim 2 \times 10^{11} M_\odot$ plus a dark matter ring at $13 < R < 18.5$ kpc with mass $\sim 2.5 \times 10^{10} M_\odot$ are required. This result is especially intriguing given other estimates for the shape of the Milky Way's halo that suggest that it could indeed be rather spherical or even prolate (e.g., Helmi 2004; Johnston et al. 2005; Law et al. 2005; Belokurov et al. 2006; Fellhauer et al. 2006). In addition, the existence of a massive dark matter disc is unexpected in the collisionless CDM paradigm. This might indicate that more physics should be added in the simulations of structure formation (e.g., baryonic physics) or the lack of complete modelling of the flaring problem.

It is commonly argued that MOND is a more falsifiable theory than CDM hypothesis because it has less adjustable parameters to fit astronomical observations. One expects that if it is not easy to explain the flaring in CDM theory, it should be even more difficult in MOND. It is interesting to see if, given the measured baryon distribution of the Milky Way, MOND is able to successfully explain the Galactic flaring.

In section 2, we discuss the vertical distribution of self-gravitating mass layers under MOND. In particular, we give the semi-analytic framework to derive the radial dependence of the thickness of the H I layer in axisymmetric galactic discs. In section 3, we apply our method to derive the expected MOND H I flaring in the Milky Way. By comparing the predictions with recent determinations of the thickness of the H I disc in the Galaxy, we are able to test the ability of MOND to reproduce the H I flaring in an extended radial range ($10 \text{ kpc} \leq R \leq 40 \text{ kpc}$).

2 FLARING OF DISCS: THEORETICAL APPROACH

2.1 Background and motivation

A possible interpretation of the missing mass in spiral galaxies is that the flatness of the rotation curves reflects a failure of the Newton law rather than the existence of vast quantities of dark matter. Milgrom (1983) suggested that for axisymmetrical systems, the *real* acceleration at the midplane of the configuration, \vec{g} , is related with the Newtonian acceleration, \vec{g}_N , by:

$$\mu(|\vec{g}|/a_0)\vec{g} = \vec{g}_N, \quad (1)$$

where a_0 is an universal acceleration of the order of $\sim 10^{-8} \text{ cm s}^{-2}$, and $\mu(x)$ is a monotonic and continuous function with the property that $\mu(x) \simeq x$ for $x \ll 1$ (deep MOND regime) and $\mu(x) \simeq 1$ for $x \gg 1$ (Newtonian regime). Although some effort has been made to derive the form of the interpolating function from basic principles (e.g., Bekenstein 2004), it is arbitrary but once it is fixed from astronomical observations, it is universal. A rather general form is

$$\mu(x) = \frac{x}{(1 + x^n)^{1/n}}, \quad (2)$$

where $n(x) > 0$ and obeys that $n'(x) \leq 0$ for $x \ll 1$ and $n'(x) \geq 0$ for $x \gg 1$. The simplest case is to assume n a positive real constant. The exponent n determines how abrupt is the transition between the Newtonian to the MOND regime. Since for $n > 2$ the interpolating functions do not differ

much, Milgrom (1983) selected $n = 2$ for simplicity. Interestingly, the standard ($n = 2$) interpolating function succeeded in fitting the rotation curves of most external galaxies, being the stellar mass-to-light ratio of the disc the only free parameter (e.g., Sanders 1996; Sanders & McGaugh 2002; Sanders 2004). Recently, Famaey & Binney (2005, hereafter FB) suggested that $n = 1$ is better for MOND to fit the inner rotation curve of the Basel model of the Milky Way (Bissantz et al. 2003). For a sample of galaxies having a gradual transition from the Newtonian limit in the inner regions to the MOND limit in the outer parts, Famaey et al. (2007) and Sanders & Noordermeer (2007) conclude that with respect to rotation curve fitting alone, there is no reason to prefer $n = 1$ to $n = 2$, it is only the plausibility of the relative M/L values for bulge and disc as well as the generally smaller global M/L , that support $n = 1$. Moreover, the best fit for the sample of Famaey et al. (2007) was obtained for $n = 1$. From the χ^2 statistics of the global fits, they derived $n \geq 0.85$ at one-sigma uncertainty. Since values $n > 2$ seem to be incompatible with the measured terminal velocities interior to the Solar circle and require disc M/L ratios slightly higher than the predictions of stellar population synthesis models (McGaugh 2005), it turns out that values in the range $0.85 \leq n \leq 2$ are allowed by current observations, with $n = 1$ the most favoured value.

The phenomenological formulation of MOND by Eq. (1) cannot be applied to an arbitrary self-gravitating system. Bekenstein & Milgrom (1984) suggested a Lagrangian theory and also a nonlinear differential equation for the nonrelativistic gravitational potential produced by a mass density distribution ρ :

$$\vec{\nabla} \cdot \left[\mu \left(\frac{|\vec{\nabla}\Phi|}{a_0} \right) \vec{\nabla}\Phi \right] = 4\pi G\rho. \quad (3)$$

Only for very special configurations (one-dimensional symmetry –spherical, cylindrical or plane symmetric systems– or Kuzmin discs) the MOND field is related to the Newtonian field by the algebraic relation Eq. (1) (Brada & Milgrom 1995). The modified Poisson equation given by Eq. (3) overcomes many of the conceptual malades of the algebraic equation but it is very difficult to solve.

In a MONDian baryonic Universe ρ is the density distribution of the seen baryonic matter. A Newtonist, who assumes that Φ solves the Poisson equation, will deduce a fictitious dark matter density:

$$\rho_{\text{dm}} = (4\pi G)^{-1} \nabla^2 \Phi - \rho. \quad (4)$$

As Milgrom (2001) demonstrated, MOND predicts for disc galaxies a distribution of fictitious dark matter that comprises a dark disc and a rounder halo. The surface density of fictitious dark matter in the disc is

$$\Sigma_{\text{dm}} = \left(\frac{1}{\mu(g^+/a_0)} - 1 \right) \Sigma, \quad (5)$$

where Σ is the real (baryonic) surface density of the disc and g^+ is the total MOND acceleration just outside the disc. At large radii where $\mu \ll 1$, the ‘dark disc’ dominates, implying that Newtonian disc-flaring analyses should indicate highly flattened oblate dark haloes. Although the initial applications of the flaring technique for NGC 891 and NGC 4244 implied highly flattened dark haloes, the gas layer flaring method does not return systematically highly flattened

haloes (Olling & Merrifield 2000; Merrifield 2002; Narayan et al. 2005 for the case of the Milky Way). The question that arises is: are the predictions of MOND compatible with measurements of the flattening of galaxies? Since it is not possible for MOND to mimic prolate dark matter haloes, a clear-cut probe of the existence of a prolate halo in an isolated galaxy would be difficult to reconcile with MOND.

2.2 Scaleheight of one-dimensional planar mass layer in deep MOND

Assuming pure planar symmetry, the only component different from zero is g_z . The vertical hydrostatic equilibrium equation is:

$$\frac{dP}{dz} = -\rho \frac{d\Phi}{dz}. \quad (6)$$

Integrating this equation from 0 to z and exploiting MOND field equation (Eq. 3), we find

$$\int_0^z \frac{dP}{dz'} dz' = -(4\pi G)^{-1} \int_0^z \frac{d}{dz'} \left(\mu \frac{d\Phi}{dz'} \right) \frac{d\Phi}{dz'} dz'. \quad (7)$$

In the deep MOND, $\mu \simeq a_0^{-1} d\Phi/dz$, and hence the RHS of the above equation can be integrated immediately:

$$P(z) - P(0) = -\frac{1}{6\pi G a_0} \left(\frac{d\Phi}{dz} \right)^3. \quad (8)$$

The value of the vertical force $d\Phi/dz$ can be inferred again from the MOND field equation after integrating it between $\pm z$, $d\Phi/dz = \sqrt{2\pi G a_0 \Sigma(z)}$, where $\Sigma(z)$ is the integrated surface density $\Sigma(z) = \int_{-z}^z \rho dz'$. Substituting this expression into Eq. (8),

$$P(z) - P(0) = -\frac{1}{3} (2\pi G a_0)^{1/2} \Sigma(z)^{3/2}. \quad (9)$$

For an isotropic and isothermal gas with one-dimensional velocity dispersion σ , the midplane pressure is $P(0) = \rho_0 \sigma^2$, where ρ_0 is the density at $z = 0$. Adopting the boundary condition $P(\infty) = 0$, we derive the pressure at the midplane:

$$\rho_0 \sigma^2 = \frac{1}{3} (2\pi G a_0)^{1/2} \Sigma_\infty^{3/2}, \quad (10)$$

with $\Sigma_\infty = \Sigma(\infty)$. When the scaleheight z_0 is defined as $z_0 \equiv \Sigma_\infty / (2\rho_0)$, it satisfies

$$z_0 = \frac{3}{2} \frac{\sigma^2}{\sqrt{2\pi G a_0 \Sigma_\infty}}, \quad (11)$$

for our isothermal self-gravitating layer in the deep MOND regime. The dependence of z_0 on Σ_∞ is obviously different than in the Newtonian case. In order to facilitate comparison it is convenient to rewrite this formula in a more familiar way exploiting the relation $\mu_\infty \equiv \mu(\infty) = a_0^{-1} \sqrt{2\pi G a_0 \Sigma_\infty}$,

$$z_0 = \frac{3}{4} \frac{\mu_\infty \sigma^2}{\pi G \Sigma_\infty}. \quad (12)$$

Therefore, the usual recipe of replacing $G \rightarrow G/\mu$ to obtain the MOND value from the Newtonian expression overestimates the scaleheight by a factor 4/3 in this case.

2.3 Infinite mass sheet in an external gravitational field

Suppose now that our mass layer is under a constant external field $\vec{g}_{\text{ext}} = (g_x, 0, 0)$ and that the dynamics is dominated by g_x , i.e. $g_x \gg g_z$, where g_z is the vertical acceleration created by the self-gravity of the layer. In that case the modified Poisson equation (Eq. 3) reads

$$\rho = (4\pi G)^{-1} \frac{d}{dz} \left(\mu \frac{d\Phi}{dz} \right), \quad (13)$$

with $\mu(g/a_0)$ and $g = (g_x^2 + g_z^2)^{1/2} \approx g_x$ in an external-dominated field. Therefore μ is constant (independent of x and z), and thus

$$\rho = \frac{\mu}{4\pi G} \frac{d^2\Phi}{dz^2}. \quad (14)$$

Following the same steps as in the previous subsection, the vertical scaleheight of the layer in an external dominated field is

$$z_0 = \frac{\mu \sigma^2}{\pi G \Sigma_\infty}. \quad (15)$$

Note that $\mu(g_x/a_0) = \text{constant}$. When $g_x \gg a_0$, we have $\mu \approx 1$ and we recover Spitzer's formula. If, on the opposite case, the layer is in the deep MOND regime ($g_z \ll g_x \ll a_0$), then $\mu \simeq g_x/a_0$ and z_0 is proportional to g_x . This result has interesting consequences in galactic discs. Consider now a region of the disc outside the central region such that $g_R \gg g_z$. If g_R is mostly determined by the inner stellar disc and g_z by the local self-gravity of the H I layer, then g_R plays the role of the external field. According to the ongoing discussion, if the adopted stellar mass-to-light ratio is increased and thus its mass, then the H I layer in that region becomes thicker. This result is reminiscent of the external field effect (Milgrom 1995) and will be relevant in §2.5.

2.4 Gravitational potential in axisymmetric thin discs

The MONDian Poisson equation (3) is difficult to solve even numerically. However, it can be simplified when studying the vertical structure of the outer parts of axisymmetric galactic discs. The field equation can be written as:

$$\mu(x) \nabla^2 \Phi + \vec{\nabla} \mu(x) \cdot \vec{\nabla} \Phi = 4\pi G \rho, \quad (16)$$

where $x = |\vec{\nabla} \Phi|/a_0$. For an axisymmetric configuration Equation (16) can be expanded in cylindrical coordinates (R, z) as:

$$\mu(x) \nabla^2 \Phi + \left(\frac{\partial \Phi}{\partial R} \frac{\partial \mu}{\partial R} \right) (1 + \xi) = 4\pi G \rho, \quad (17)$$

where

$$\xi = \xi_\Phi \xi_\mu \quad (18)$$

with

$$\xi_\Phi(R, z) = \left(\frac{\partial \Phi}{\partial z} \right) \left(\frac{\partial \Phi}{\partial R} \right)^{-1} = \frac{g_z}{g_R}, \quad (19)$$

and

$$\xi_\mu(R, z) = \left(\frac{\partial \mu}{\partial z} \right) \left(\frac{\partial \mu}{\partial R} \right)^{-1} = \left(\frac{\partial g}{\partial z} \right) \left(\frac{\partial g}{\partial R} \right)^{-1}. \quad (20)$$

Note that in a smooth disc galaxy $g_R < 0$, and $\partial g/\partial R < 0$ (see the Appendix), whereas $\text{sign}(g_z) = -\text{sign}(\partial g/\partial z) = -\text{sign}(z)$, implying $\xi < 0$. No approximations at all have been made so far, and Eq. (17) is fully equivalent to the original one for axisymmetric systems.

The factor $\frac{\partial \Phi}{\partial R} \frac{\partial \mu}{\partial R}$ in Eq. (17) can be rewritten as:

$$\frac{\partial \Phi}{\partial R} \frac{\partial \mu}{\partial R} = \frac{d\mu}{dx} \frac{\partial \Phi}{\partial R} \frac{\partial x}{\partial R} \simeq \frac{1}{a_0} \frac{d\mu}{dx} \frac{\partial \Phi}{\partial R} \frac{d}{dR} \left(\frac{v_c^2}{R} \right). \quad (21)$$

In the last equality we have used that $\xi_\Phi \ll 1$ within H I galactic discs (see the Appendix), so that $x \equiv |\vec{\nabla} \Phi|/a_0 = x(R, 0) \sqrt{1 + \xi_\Phi^2} \simeq x(R, 0) = v_c^2(R, 0)/(Ra_0)$. Using that

$$\nabla^2 \Phi = \frac{1}{R} \frac{\partial}{\partial R} \left(R \frac{\partial \Phi}{\partial R} \right) + \frac{\partial^2 \Phi}{\partial z^2} = \frac{1}{R} \frac{\partial v_c^2}{\partial R} + \frac{\partial^2 \Phi}{\partial z^2}, \quad (22)$$

we are lead to the final modified Poisson equation under MOND dynamics:

$$\mu \frac{\partial^2 \Phi}{\partial z^2} = 4\pi G \rho - (1 + \xi) \frac{v_c^2}{a_0 R} \frac{d\mu}{dx} \frac{d}{dR} \left(\frac{v_c^2}{R} \right) - \frac{\mu}{R} \frac{dv_c^2}{dR}, \quad (23)$$

where $v_c^2 \equiv v_c^2(R, 0)$ is the circular velocity at the midplane of the disc. Or, equivalently,

$$\frac{\partial^2 \Phi}{\partial z^2} = 4\pi \frac{G}{\mu} \rho - (1 + \xi) L(x) \frac{d}{dR} \left(\frac{v_c^2}{R} \right) - \frac{1}{R} \frac{dv_c^2}{dR}, \quad (24)$$

where $L(x) = d \ln \mu / d \ln x \geq 0$ is the logarithmic derivative of μ at the same value of the argument. For a nearly constant rotation curve, the third term of the RHS is very small. Combining Eq. (24) with the hydrostatic equilibrium equation (Eq. 6), one can obtain the vertical distribution for an isothermal disc.

2.5 Interpretation of the modified Poisson equation

In order to gain some insight, below we compare the different terms of Eq. (24) with the corresponding terms in the Newtonian equation. For an axisymmetric disc, the Newtonian Poisson equation is

$$\frac{\partial^2 \Phi}{\partial z^2} = 4\pi G \rho - \frac{1}{R} \frac{dv_c^2}{dR}. \quad (25)$$

The equation above has been used vastly to study the vertical equilibrium in the standard dark matter scenario (e.g., Olling 1995, 1996; Olling & Merrifield 2000; Narayan et al. 2005). Obviously, the Newtonian equation can be recovered from the MONDian equation taking the limit $a_0 \rightarrow 0$. In fact, in the Newtonian limit, $\mu \rightarrow 1$, $d\mu/dx \rightarrow 0$, hence $L(x) \rightarrow 0$ and Eq. (24) simplifies to Eq. (25).

Comparing Eqs (24) and (25), we see that in the MOND case, the surface density is replaced by the effective surface density Σ/μ , as expected from our discussion in sections 2.1 (see Eq. 5) and 2.3. The confining effect of this term is inversely proportional to μ . As anticipated in section 2.3, if we increase the stellar mass of the disc by adopting a bit larger stellar mass-to-light ratio, the rotation velocity v_c will increase correspondingly and hence, the effective gravitational constant $G/\mu \propto G/v_c^2$ becomes smaller at these radii.

Interestingly, Eq. (24) contains a term proportional to $L(x)$; we will refer to it as the L -term. In principle, this term has no analog in Newtonian dynamics. In order to understand its nature, consider the region of a certain galaxy

where the rotation curve is flat, i.e. $v_c(R) = \text{const}$, and write Eq. (24) in terms of the vertical and angular frequencies:

$$\nu^2 = 4\pi \frac{G}{\mu} \rho + (1 + \xi) L(x) \Omega^2, \quad (26)$$

where $\Omega(R) = v_c/R$. The L -term becomes important in the vertical equilibrium configuration when

$$(1 + \xi) \mu(x) L(x) \Omega^2 \gtrsim 4\pi G \rho. \quad (27)$$

Certainly, the L -term is crucial when the centripetal acceleration is sufficiently low that we are in the MOND regime, $\mu(x) \approx x$, and for midplane densities lower than the critical density given by:

$$\rho_c(R) = (1 + \xi) \frac{v_c^2}{Ra_0} \frac{\Omega^2}{4\pi G}. \quad (28)$$

Since the asymptotic velocity in MOND is $v_c^4 = GMa_0$, where M is the total mass of the disc, the critical density can be rewritten as $\rho_c(R) = (1 + \xi) M/(4\pi R^3)$.

As a reference number, the critical density for a galaxy with $v_c = 220 \text{ km s}^{-1}$ is $2.3(1 + \xi) \times 10^{-3} \text{ M}_\odot \text{ pc}^{-3}$ at $R = 20 \text{ kpc}$. For Galactic parameters, we find that $|\xi| \approx 0.03$ at 20 kpc (using our estimate, Eq. (A6), with a HWHM scale $h = 500 \text{ pc}$ and $\sigma = 9 \text{ km s}^{-1}$). Since the midplane H I volume density at 20 kpc is $\sim 0.9 \times 10^{-3} \text{ M}_\odot \text{ pc}^{-3}$, we expect the L -term to be important or even dominant at the very outer disc, say $R \gtrsim 20(v_c/220 \text{ km s}^{-1}) \text{ kpc}$. At these radii, ξ can be neglected as compared to 1 and Eq. (26) can be written as:

$$\nu^2 = 4\pi \frac{G}{\mu} \sum_{i=1}^3 \rho_i + \Omega^2, \quad (29)$$

where we have explicitly quoted that the baryonic density is the sum of three components, the stellar, atomic (He corrected) and molecular hydrogen mass densities. Stubbs & Garg (2005) have proposed to use jointly the rotation velocity and velocity dispersion of galactic discs to test the self-consistency of MOND. From our analysis, we learn that μ can be derived from the observed vertical velocity dispersion σ_z , the scaleheight of the disc h and the surface density Σ , according to the following relation

$$\sigma_z^2 = \pi \frac{G}{\mu} \Sigma h + \frac{1}{2} L(x) \Omega^2 h^2. \quad (30)$$

2.6 L-term and the dark matter halo

Imagine a Newtonist and a MONDianist trying to explain the dynamics of a particular galaxy, i.e. the same Φ . Since they use different field equations, they infer different mass distributions. Newtonists add a spherical dark halo of the form

$$\rho_h(r) \approx \frac{v_c^2}{4\pi G r^2} \quad (31)$$

to explain the flatness of the rotation curves in the outer parts of disc galaxies. In the following we argue that the L -term is the MOND counterpart of the Newtonian spherical dark halo. We start noting that, with this dark halo, the conventional Poisson equation at large radii reads:

$$\frac{\partial^2 \Phi}{\partial z^2} = 4\pi G \left(\sum_{i=1}^3 \rho_i + \rho_h \right). \quad (32)$$

Substituting for ρ_h into Eq. (32) with $v_c^2 = \Omega^2 r^2$ we obtain

$$\frac{\partial^2 \Phi}{\partial z^2} = 4\pi G \sum_{i=1}^3 \rho_i + \Omega^2, \quad (33)$$

or written in terms of the frequencies:

$$\nu^2 = 4\pi G \sum_{i=1}^3 \rho_i + \Omega^2. \quad (34)$$

Comparing Eqs (29) and (34) we see that, in the outer parts of galaxies where the dynamics is in the deep MOND regime, the L -term mimics the vertical pull created by the spherical dark halo in the traditional Newtonian scenario (see also Milgrom 2001). In summary, MOND predicts for disc galaxies a fictitious round dark halo and a fictitious dark disc. The resultant flattened potential along the vertical axis implies that, if MOND is correct, Newtonists should only infer *oblate* dark matter haloes around disc galaxies. The inference of prolate ($q > 1$) dark haloes in isolated spiral galaxies would suffice to rule out ‘classical’ MOND. Of course, MOND is not fundamentally incompatible with the existence of unseen matter and one might argue that an unseen prolate spheroid of stars can account for the Newtonian inference of a prolate dark halo, but this would weaken its appeal.

3 APPLICATION: THE MILKY WAY

One advantage of studying our Galaxy as compared to other external galaxies is that we know quite well its baryonic mass. For no other galaxy do we have information of comparable quality. Using the terminal velocities, Famaey & Binney (2005) were able to put constraints on the form of the interpolating function given the measured baryon distribution. In addition, the new All Sky H I Survey (the Leiden-Argentine-Bonn [LAB] survey as it is known; Kalberla et al. 2005) provides us a reliable three dimensional structure of the H I disc of the Milky Way up to a minimum of 40 kpc from the Galactic centre. Currently, this is the most sensitive Milky Way H I line survey with the most extensive coverage both spatially and kinematically. Since the stellar contribution drops down rapidly in the outer region, this huge H I disc can serve as an excellent probe for testing alternative theories to dark matter and thereby the nature of gravity. In this analysis we use MOND (as opposed to dark matter) as a possible candidate for reproducing the thickness of the H I layer of our Galaxy and hence test its standpoint in this regard.

3.1 The method

We have derived the vertical distribution of the H I layer following the same simplifying assumptions than in the standard procedure implemented in Olling (1995). The system is assumed to be in a (perhaps turbulent) steady state which can be described by a Jeans-like equation. The velocity dispersion tensor of the gas, which includes thermal and macroscopic gas motions, is assumed to be round and constant (isothermal) with z as well as R . The maps of the second moment (or velocity dispersion) in external galaxies display a patchy distribution (e.g., Petric & Rupen 2007) with regions of relatively low velocity dispersion (5 km s^{-1}) and

high velocity dispersion (12 km s^{-1}). Therefore, the assumption of constant velocity dispersion should be reasonable after averaging over azimuth. Under these assumptions, the thickness of the Milky Way’s gas layer is dictated by the hydrostatic balance between the pull of gravity toward the Galactic plane and the pressure forces acting on the gas:

$$\sigma_i^2 \frac{\partial \rho_i}{\partial z} = -\rho_i \frac{\partial \Phi}{\partial z}. \quad (35)$$

If the interstellar gas is in the form of small dense clumps, the vertical component of its velocity dispersion should be smaller than the radial component, in the same manner than stars. Even so, the term due to the tilt of the velocity dispersion tensor is expected to be very small (Olling 1995; Becquaert & Combes 1997; Kalberla 2003). The gradient of the mean pressure of the hot gas ($T > 10^5 \text{ K}$) is negligible within the thickness of the the H I disc because the scaleheight of hot gas is much larger than the scaleheight of H I. For instance, the decrease of hot gas density away from the plane is consistent with a local scaleheight of 3.2 kpc. Overpressured bubbles of hot gas formed by supernovae explosions may be a source of driving porosity in the ISM and turbulent motions in the H I. Porosity may modify the hydrostatic properties of the gas layer. However, for a turbulent ISM, the effect of the hot medium pressure is essentially included in the *turbulent* velocity dispersion.

To follow the standard technique as close as possible in order to facilitate comparison with previous work, the magnetic and cosmic ray pressures are neglected. This is probably the most fragile assumption. To separate variables, we will postpone investigating the effects of non-thermal pressure terms until section §3.5.2.

Equation (35) must be solved under boundary conditions at high z , which are given by the properties of the embedding ambient medium. One can see that reasonable hot halo components in hydrostatic equilibrium, as that derived by Benjamin & Danly (1997), have little impact on the H I scaleheight. Not only the pressure by the hot halo gas but also any ram pressure exerted by the intergalactic medium onto the disc is also thought to have an ignorable effect on the vertical distribution of the H I layer.

To date, most authors have adopted these assumptions to determine the distribution of the gas (e.g., Olling 1995, 1996; Becquaert & Combes 1997; Olling & Merrifield 2000; Narayan & Jog 2002; Kalberla 2003; Narayan et al. 2005; Abramova & Zasov 2007). Although the limitations of these suppositions are well-documented in the literature, the reader is referred to §3.5 for a discussion.

3.2 Mass model

In order to estimate the thickness of the H I layer, the circular velocity should be known (see Eq. 24). Given the measured baryon distribution, the circular velocity can be determined. In this sense, MOND has less free parameters than the hypothesis of dark haloes. We consider the Galaxy to be composed of a bulge, a stellar disc and ISM in the form of H I and H₂ layers. For our Galaxy they are all based on well-known observations as described below. Our analysis treats the gas and the stars as axisymmetric distributions. Therefore, the resulting quantities should be considered as average values over azimuth.

3.2.1 Stellar components

The density profile of the bulge is assumed to be described by a spherical Plummer-Kuzmin model:

$$\rho_b(r) = \frac{3M_b}{4\pi R_b^3} \left(1 + \frac{r^2}{R_b^2}\right)^{-5/2}, \quad (36)$$

where the bulge mass $M_b = 3.2 \times 10^{10} M_\odot$ and the bulge scalelength $R_b = 2.5$ kpc. Inclusion of this simple bulge reproduces a reasonable looking rotation curve of the Galaxy. The contribution of the bulge to the H I scaleheight in the outer parts ($R > 10$ kpc) of the Galaxy is negligible. For instance, for a mass $M_b = 1.5 \times 10^{10} M_\odot$ (e.g., Flynn et al. 2006), the scaleheight changes $< 4\%$.

The stellar disc is modelled as an exponential surface density distribution with a central surface density Σ_0 and disc scalelength R_d such that:

$$\Sigma_\star(R) = \Sigma_0 e^{-R/R_d}, \quad (37)$$

where $\Sigma_0 = 640.9 M_\odot \text{pc}^{-2}$ and $R_d = 3.2$ kpc (Mera et al. 1998; López-Corredoira et al. 2002; Larsen & Humphreys 2003; Sommer-Larsen et al. 2003), implying a total stellar mass of $4.1 \times 10^{10} M_\odot$ in the disc. The local stellar surface density (at $R = R_\odot = 8.5$ kpc) turns out to be $45 M_\odot \text{pc}^{-2}$, which when combined with the corresponding value for gas (H I + H₂) of $7 M_\odot \text{pc}^{-2}$, gives the total local surface density inferred by most observations (e.g., Holmberg & Flynn 2004). The vertical velocity dispersion of the stars as a function of R is taken from Lewis & Freeman (1989).

3.2.2 Gaseous components and the flaring of the H I layer

The H I surface density (He corrected¹) as a function of the galactocentric radius is taken as an input for the disc model. As said before, the H I data comes from the most recent comprehensive H I survey of our Galaxy, the LAB survey (Kalberla et al. 2005). Here we use the average observed flaring (of North and South hemispheres) results for a flat rotation curve with $v_c = 220 \text{ km s}^{-1}$ and $R_\odot = 8.5$ kpc (the current IAU standard values), to compare with the predicted scaleheight in MOND.

The vertical velocity dispersion of H I, σ_{HI} , outside the solar circle is hard to measure, and so not yet known. Observations of external galaxies imply that σ_{HI} is typically constant along galactocentric radius with a value $7\text{--}9 \text{ km s}^{-1}$ (e.g., Sellwood & Balbus 1999), or declines slightly with radius (Dib et al. 2006, and references therein). Since in the inner Galaxy the H I is observed to have a velocity dispersion of $9.2 \pm 1 \text{ km s}^{-1}$ independent of radius (Malhotra 1995) and since there is evidence that the velocity dispersion in the outer Galaxy equals the value inside the solar circle (Blitz & Spergel 1991), Olling & Merrifield (2000, 2001) assumed a constant σ_{HI} of 9.2 km s^{-1} as a more likely value. However, a slightly declining velocity dispersion could also be admissible. In order to calculate the scaleheight we consider models across a range of values $7 \text{ km s}^{-1} \leq \sigma_{\text{HI}} \leq 9 \text{ km s}^{-1}$, constant with radius.

The H₂ surface density as a function of R was taken

from Wouterloot et al. (1990) and its vertical velocity dispersion is 5 km s^{-1} (Clemens 1985).

3.3 MOND parameters and the rotation curve

Milgrom's formula (Eq. 1) has been used extensively to fit the rotation curves of external galaxies. The MOND circular speed v_c in the disc mid-plane is related to its Newtonian counterpart (without any dark matter), $v_{c,N}$, by the following equation:

$$\mu(x)v_c^2 = v_{c,N}^2 \quad (38)$$

(Brada & Milgrom 1995) where $x = v_c^2/(Ra_0)$ and the Newtonian rotation speed in the mid-plane of the Galaxy is given by:

$$v_{c,N}^2 = v_{\text{disc}}^2 + v_{\text{bulge}}^2 + v_{\text{gas}}^2. \quad (39)$$

For a set of external galaxies with high quality rotation curves, Begeman et al. (1991) derived $a_0 = (1.2 \pm 0.27) \times 10^{-8} \text{ cm s}^{-2}$. This has been the preferred value for MOND studies that followed (Sanders & Verheijen 1998; Famaey & Binney 2005). However, Bottenga et al. (2002) argue based on Cepheid-based distance scale to UMa cluster of galaxies that the value of a_0 should be adjusted to $0.9 \times 10^{-8} \text{ cm s}^{-2}$. Adopting the mass model described in §3.2 and the relation between the Galactic constants, $\Theta_0/R_\odot = (27 \pm 2.5) \text{ km s}^{-1} \text{ kpc}^{-1}$ (Kerr & Lynden-Bell 1986; Reid et al. 1999), reasonable rotation curves are generated for a_0 in the range of 0.8×10^{-8} to $1.2 \times 10^{-8} \text{ cm s}^{-2}$. Figure 1 shows the rotation curves for the interpolating functions with $n = 1$ and $n = 2$ and different a_0 . The radial upper limit of 40 kpc is set by the reliability of H I data. At the solar point $R_\odot = 8.5$ kpc, the circular speed lies in the range of 215 to 243 km s^{-1} , conforming with the accepted range of ratio of Galactic constants. This implies that the model parameters assumed above are appropriate. Note that the differences in the rotation curves are small at large radii because the asymptotic value of the rotation speed is given by $v_c(\infty) = (GMa_0)^{1/4}$ for both interpolating functions.

We like to point out that the assumed rotation curves behind the theoretical and observed scaleheight curves do not exactly match. In the case of H I observations, the conversion of brightness temperature T_B , to volume density depends on the assumed distance to the Galactic centre R_\odot , the local rotation velocity v_\odot and the outer rotation curve. The conventional way to go with LAB survey analysis is to assume a flat rotation curve of 220 km s^{-1} with $R_\odot = 8.5$ kpc. The scaleheight data used in this paper is based on these values, whereas the rotation curves used to estimate the theoretical flaring are based on the adopted mass model of our Galaxy. Ideally, we should use rotation curves in Fig. 1 to analyse the LAB data. However, the difference between the two is only 10% – 15% and we will see that, for our purposes here, the results are stable against such modest adjustments. So its effect on the scaleheight will not compromise our conclusions.

3.4 H I scaleheight in the Galaxy with MOND

Using Runge-Kutta method, we solve equations (24) and (35) numerically as an initial value problem to obtain our

¹ Our analysis does include a 30% per cent contribution by mass from helium.

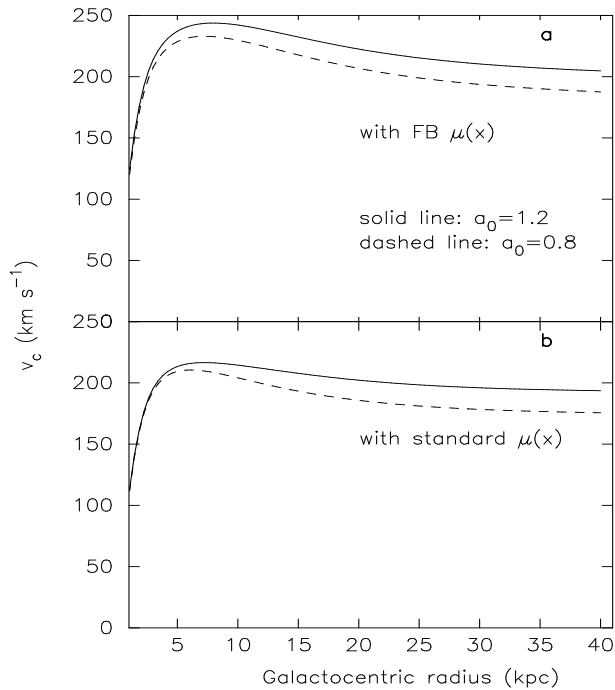


Figure 1. Rotation velocity curves for different a_0 , in units of $10^{-8} \text{ cm s}^{-2}$, and for the FB (panel a) and standard (panel b) interpolating functions. Note that the circular speed v_c is slightly higher for the FB interpolating function. MOND produces a falling rotation curve in the region of interest ($R > 10 \text{ kpc}$).

object of interest: density as a function of z at different R . Readers are referred to Narayan & Jog (2002) for a detailed numerical procedure. As discussed in §2.5, we can neglect ξ as compared to 1 in Eq. (24) in the whole range of interest ($10 \text{ kpc} \leq R \leq 40 \text{ kpc}$) because at large radii where the L -term is important, $\xi \lesssim 0.04$ (see the Appendix). In this way we obtain the simultaneous vertical density distributions of stars, H I and H₂.

The vertical density distributions of stars and H I for $\sigma_{\text{HI}} = 7 \text{ km s}^{-1}$, $n = 1$ and $a_0 = 1.2 \times 10^{-8} \text{ cm s}^{-2}$ are shown in Fig. 2. Even though we have three disc components (stellar disc, H I and H₂ layers) having different vertical velocity dispersions and gravitationally coupled under MOND, the vertical density profiles are still very close to a sech^2 -function. As expected, the H₂ layer is the most compact one followed by the H I layer and the stellar disc, respectively (see Fig. 2, upper panel). The scene is different at large distances from the Galactic centre. The azimuthally averaged H₂ surface density is so low there that it becomes incorrect to assume it as a continuous layer. It may exist as rare clouds and so disappear from our picture.

By solving the equations at regular R intervals (between 10–40 kpc), the scaleheight h , defined as the HWHM of the vertical H I density distribution², can be plotted as a function of R (Fig. 3). The H I layer undergoes flaring due to a combination of decreasing total surface density and a steady velocity dispersion of 7 km s^{-1} , and therefore extends verti-

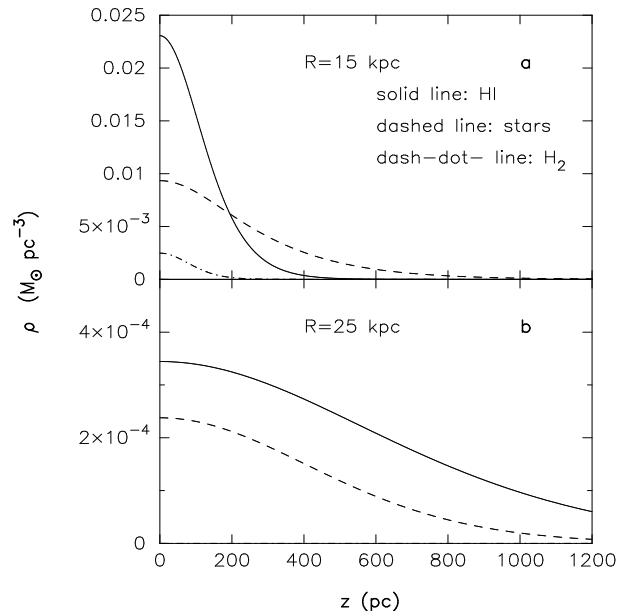


Figure 2. Density distribution along the vertical direction for H I, stars and H₂ in the outer parts of the Galactic disc according to MOND for $\sigma_{\text{HI}} = 7 \text{ km s}^{-1}$, $a_0 = 1.2 \times 10^{-8} \text{ cm s}^{-2}$ and $n = 1$.

cally beyond the stellar disc. The L -term in Eq. (24) becomes similar to the local self-gravity term, $4\pi\mu^{-1}G\rho$, at $\sim 27 \text{ kpc}$. At $R = 40 \text{ kpc}$ it turns out to be 4 times larger than the local self-gravity when the FB interpolating function and $a_0 = 0.8 \times 10^{-8} \text{ cm s}^{-2}$ are used. While the differences in the flaring between the standard and the FB interpolating functions are not significant beyond $R = 27 \text{ kpc}$, the standard interpolating function predicts a thicker H I disc at $10 \text{ kpc} < R < 20 \text{ kpc}$ (see §3.5.3 below). For $n = 2$, $a_0 = 1.2 \times 10^{-8} \text{ cm s}^{-2}$ and $\sigma_{\text{HI}} = 7 \text{ km s}^{-1}$, MOND predicts a scaleheight of $\sim 375 \text{ pc}$ at $R = 20 \text{ kpc}$ and $\sim 1625 \text{ pc}$ at $R = 40 \text{ kpc}$.

Now we make a one-to-one comparison between the predicted and the observed scaleheights of H I from the LAB survey. This comparison is possible only for the H I layer because the number counts of both stars and molecular hydrogen fizzle out at such large radii. The circles in Figs. 3 and 4 represent the H I scaleheight from the LAB survey data as derived in the reference model (see §3.2.1 in Kalberla et al. 2007). For the adopted σ_{HI} , the predicted MOND scaleheight always falls below the LAB values in the entire range considered. Close to 10 kpc, the predicted value is almost 60% below the observed value and at 40 kpc it is about 30% less. The lower a_0 slightly lifts the curve up but the discrepancy at the interval $10 \text{ kpc} < R < 17 \text{ kpc}$ and beyond 30 kpc still remains.

The velocity dispersion in our Galaxy is, of course, uncertain. In the inner Galaxy, the H I is observed to have a velocity dispersion of $9.2 \pm 1 \text{ km s}^{-1}$, independent of radius (Malhotra 1995). If we assume that this value characterizes the turbulent motions of the gas throughout the Galaxy, the flaring of the H I layer can be reproduced well at $R \gtrsim 17 \text{ kpc}$ (see Fig. 4). At $25 \text{ kpc} \leq R \leq 32 \text{ kpc}$, the predicted flaring curve moves away from the observed one by less than 15%. Due to the fact that the flaring in the northern hemisphere is $\sim 80\%$ larger than in the southern hemisphere,

² Note that the definitions of z_0 and h are different. In this section, it is more convenient to use h .

the mentioned discrepancy of 15% can be attributed to our axisymmetric assumption. It is important to note that the L -term and the local self-gravity term vary having a different radial dependence and should work out in phase to explain the flaring curve. If the L -term were not included, MOND would overestimate the thickness of the H I disc beyond ~ 25 kpc. In particular, it would be overestimated by a factor of 5 at $R = 40$ kpc. The success of MOND in predicting the H I flaring at the outer parts is noteworthy because at such large radii the predictions are very robust to small adjustments on the Galactic mass model, Galactic constants, the value of a_0 or the index n of the interpolating function (see, for instance, Fig. 3). The thickness is essentially determined by the adopted σ_{HI} . If a H I velocity dispersion of ≈ 9 km s $^{-1}$ is taken at face value, the observed H I data up to 40 kpc seems to favour the lowest acceptable values of the universal acceleration $a_0 \sim 0.8 \times 10^{-8}$ cm s $^{-2}$.

In Fig. 4 we see that the observed thickness at 10 kpc $\lesssim R \lesssim 15$ kpc is still a factor of 1.7 larger as compared to the MOND prediction. This factor cannot be attributed to the approximations we made in the derivation of Eq. (24). It is also unlikely that systematic deviations from axisymmetry can account for that difference because the average thickness over $0^\circ < \phi < 180^\circ$ is similar to the average value over $180^\circ < \phi < 360^\circ$ at the interval $10 \text{ kpc} \leq R \leq 15 \text{ kpc}$ (Levine et al. 2006a; Kalberla et al. 2007).

It should be borne in mind that the flaring curve and the H I volume density as inferred from the LAB data are dependent on the Galactic constants and the adopted rotation curve and we pick up the $v_c = 220$ km s $^{-1}$ reference model. Nevertheless, we established, after some investigation, that the above mentioned discrepancy between the predictions and observations cannot be smeared out by slightly changing the values of R_\odot and v_\odot , or by adopting the rotation curves of Fig. 1 to analyse the LAB data. In order to sort through a large parameter space, we look at other parameters that do not appear to be strongly constrained by the data; this will be done in the next section.

3.5 Effects of incomplete modelling and other uncertainties

In the previous section it was found that in the MOND formulation the observed disc material gives rise to too thin a thickness at $10 \text{ kpc} \leq R \leq 15 \text{ kpc}$. In order to determine the implications of this result, we need to consider effects of incomplete modelling and other uncertainties.

3.5.1 The stellar mass-to-light ratio

As already said, the L -term is small as compared to the self-gravity term in the “inner” disc ($R \leq 20$ kpc), implying that $h \propto \mu/\Sigma$. It is possible to have a thicker H I disc in the inner disc if Σ is decreased simply by decreasing the stellar mass-to-light ratio³ Υ . In fact, if Υ is decreased, the circular

velocity and thus μ lower but the drop in μ is not enough to compensate the reduction on Σ . In particular, if we take the FB interpolating function with $a_0 = 0.8 \times 10^{-8}$ cm s $^{-2}$ and reduce Υ to a value such as that $v_\odot = 200$ km s $^{-1}$, which is quite low but still compatible with the terminal velocity data (Famaey & Binney 2005), h increases about 27% at $R = 15$ kpc and about 10% at $R \gtrsim 35$ kpc. Therefore, the fit is globally better in the latter case but the overcorrection is not eliminated.

3.5.2 Non-thermal pressure terms

A velocity dispersion σ_{HI} of ~ 9 km s $^{-1}$ may be attributed to the gas random motions. Potentially, there may be other forces helping to support the H I layer as cosmic rays and magnetic fields, which lead to a larger *effective* velocity dispersion σ'_{HI} (e.g., Parker 1966; Spitzer 1978; Boulares & Cox 1990). The variation with radius in the pressure support from magnetic fields and cosmic rays is essentially unconstrained. The simplest assumption is that, like the turbulent pressure, these two terms do not vary with radius and so the effective velocity dispersion is a constant. Following Spitzer (1978), denote by α_B the ratio between the magnetic pressure arising from the regular field P_B and the kinetic pressure P_g . Similarly, we introduce $\alpha_b \equiv P_b/P_g$ and $\alpha_{CR} \equiv P_{CR}/P_g$, where P_b is the pressure arising from the random field and P_{CR} the pressure due to cosmic rays. The scaleheights of the non-thermal pressure terms are κ_B , κ_b and κ_{CR} times larger than the gaseous scaleheight. With this notation, the relative increase in the velocity dispersion is

$$\frac{\sigma'_{\text{HI}}}{\sigma_{\text{HI}}} = \sqrt{1 + \frac{\alpha_B}{\kappa_B} + \frac{\alpha_b}{\kappa_b} + \frac{\alpha_{CR}}{\kappa_{CR}}} \quad (40)$$

(e.g., Olling & Merrifield 2001). Models and observations of the ISM in the solar vicinity and external galaxies are compatible with approximate equipartition between the energy density of the turbulent magnetic field and the turbulent energy density of the gas (e.g., Zweibel & McKee 1995; Beck et al. 1996; Beck 2001; Fletcher & Shukurov 2001; Beck 2007), hence $\alpha_b \simeq 0.3$ – 0.5 (see also Kalberla & Kerp 1998). Observational constraints on the magnetic field near the Sun yield $1 \lesssim b/B \lesssim 3$ (e.g., Fletcher & Shukurov 2001 and references therein), thus $\alpha_B = 0.05$ – 0.5 . Equipartition arguments suggest the cosmic ray pressure to be equal to the total magnetic pressure, implying $\alpha_{CR} \simeq 0.5$ – 0.7 . The vertical distribution of the non-thermal components are even more difficult to obtain than is that of the gas components of the ISM. If the turbulent magnetic field has the same origin than the turbulent motions, $\kappa_b = 1$. For the regular magnetic atmosphere $\kappa_B = 5$ – 10 are reasonable values. The possible values of κ_{CR} can be derived by noting that the cosmic ray pressure is equal to the total magnetic pressure.

Using Eq. (40) with the above range of parameters we obtain $\sigma'_{\text{HI}}/\sigma_{\text{HI}} = 1.2$ – 1.4 . This is in accordance to the results of Kalberla & Kerp (1998) who conclude that $\sigma'_{\text{HI}}/\sigma_{\text{HI}} \approx 1.15$ due to the turbulent magnetic field component, when the pressure contribution from cosmic rays is not included. Ratios $\sigma'_{\text{HI}}/\sigma_{\text{HI}} \approx 1.4$ are commonly used in the literature (e.g., Sellwood & Balbus 1999; Elmegreen & Hunter 2000).

³ The associated error in the local column density of stars is ~ 10 M $_\odot$ pc $^{-2}$ (Flynn & Fuchs 1994; Holmberg & Flynn 2004). In addition, strong departures from axisymmetry could mean that the local surface density may not be representative of the azimuthally averaged value.

Since the discrepancy in the scaleheight is 25%–70%, depending on the adopted values of n and Υ , values of $\sigma'_{\text{HI}}/\sigma_{\text{HI}} = 1.12\text{--}1.3$ are required to account for the thickness of the disc at $10 \text{ kpc} \leq R \leq 15 \text{ kpc}$. We conclude that, given the uncertainties, simplified estimates indicate that non-thermal pressure support could be sufficient. Beyond the optical radius $\sim 15 \text{ kpc}$, where star formation is almost nonexistent, energy input into cosmic rays and magnetic fields from stellar sources is likely to be unimportant. Hence, a decreasing σ'_{HI} with R is expected.

3.5.3 Form of the interpolating function

In section 2.1, it was said that analyses of the rotation curves of our Galaxy and other external galaxies constrain the exponent n of the interpolating function in the range $0.85 \leq n \leq 2$. Whilst at the far outer disc $R > 27 \text{ kpc}$ the thickness of the H I disc remains almost unchanged when n is varied between 0.85 and 2, the flaring of the disc in the inner disc ($10 \text{ kpc} < R < 20 \text{ kpc}$) scales approximately as $h \propto \mu$ and so that it depends on the adopted value of n . Once the baryonic mass distribution is known, the ratio between scaleheights derived with $n = 2$ and $n = 1$ in the inner disc is:

$$\frac{h(n=2)}{h(n=1)} = \sqrt{2} \frac{(\sqrt{1+4y^2} - 1)^{1/2}}{\sqrt{1+4y} - 1}, \quad (41)$$

where $y = (v_{c,N}^2/Ra_0)^{-1}$. In the range of interest we have $y \gtrsim 1$ implying that the scaleheight is about 25% larger when the standard interpolating function is used than in the FB case. Consequently, MOND requires less non-thermal support, $\sigma'_{\text{HI}}/\sigma_{\text{HI}} \simeq 1.18$ for our standard set of parameters described in §3.2, to explain the observed flaring if the standard interpolating function ($n = 2$) is adopted.

3.5.4 Outer spiral arms and warps

It is possible that the H I layer is slightly out of hydrostatic equilibrium because of the warp and the presence of outer spiral arms. The scattering of stars and compact clouds by the spiral arms hardly increases their vertical velocity dispersion (e.g., Jenkins & Binney 1990). However, if the H I layer behaves as a smooth disc of gas, it develops a combination of a shock and a hydraulic jump; the gas may shoot up to higher z (e.g., Gómez & Cox 2002, 2004). Nevertheless, the arms outside the corotation radius are likely weak and these vertical complications are expected to occur along a thin (a few hundred parsecs) region downstream the shock/jump of the arm. The observed correlation between the maps of H I thickness and surface density –regions of higher surface density having a more reduced thickness– (Levine et al. 2006b), suggests that hydrostatic equilibrium is a good approximation. By averaging over azimuth, the alteration of the vertical structure by this jump/shock should not be significant.

It is well-known that the H I disc of the Galaxy is warped. A warp is essentially a vertical $m = 1$ mode that is maintained by some external driving force. The S-shape of the warp does not affect appreciably the local self-gravity in the disc because the wavenumber of the warp $k \ll 2\pi/h$. Since the orbit of a parcel of the disc is inclined to its

galaxy’s equatorial plane, its height z above this plane oscillates around $z = 0$ with amplitude $h_w(R)$. It is important to know at what extent this oscillatory motion may generate vertical compressions or decompressions and produce an azimuthal dependence on the thickness of the H I disc. First, compressions should induce a pressure gradient in the vertical direction of the disc (probably a shock wave or compression front) and, consequently, a characteristic asymmetric vertical morphology is expected (Sánchez-Salcedo 2004). By contrast, the observed fairly symmetric distribution of the Galactic warp suggests that the gas layer moves vertically in a solid-like fashion, as if it were incompressible. This solid-like behaviour is expected either if the bending modes are long-lived eigen-modes or they are excited by gravitational torques⁴. Just for illustration, let us consider the tidal excitation as the mechanism responsible for maintaining the warp with amplitude $h_w(R)$. The gravitational perturber (e.g., the Magellanic Clouds) may exert a tidal stretching on the disc, but this effect is very small across the thickness of the H I disc and hence we only need to study the restoring gravitational force that pulls the gas back to the disc midplane. For low amplitudes of the warp $h_w/R \ll 1$, the underlying gravitational restoring force due to the disc is described by an harmonic potential, $\Phi(z) = \nu^2 z^2/2$ with ν the vertical frequency derived in §2.5. Under this potential, one can show that the oscillatory mode in the vertical direction occurs at constant thickness. In fact, denoting by $\rho_{eq}(z)$ the hydrostatic density profile in the absence of the warp, the density $\rho(z, t) = \rho_{eq}(\tilde{x})$ with $\tilde{x} = z - h_w \cos(\nu t + \xi)$ describes an exact solution of the isothermal Jeans vertical equation for any value of the gas velocity dispersion. Since this ‘rigid’ mode is reached in a dynamical timescale Ω^{-1} , a net departure from Jeans hydrostatic equilibrium because of the warping should be small. This ‘incompressible’ behaviour has been confirmed numerically even in the case that the disc evolves only through its own gravity (see, e.g., §4 in Masset 1997).

3.5.5 Ram pressure and cold gas accretion

The ram pressure due to infalling diffuse material from the intergalactic medium could compress the disc vertically (Sánchez-Salcedo 2006). The dynamical collapse time for the H I layer is so short that Eq. (35) is still valid but should be solved with appropriate boundary conditions. What we have found is that MOND does not require any hypothetical and unseen compression by smooth intergalactic accretion flows.

The Galactic disc is probably subject to a continuous process of circulation of gas and accretion of material through condensing halo gas. The continuous infall of high velocity clouds onto the H I disc may produce enough agitation in the interstellar medium to explain the observed levels of turbulence at the outer parts (Santillán et al. 2007; Booth & Theuns 2007). Even in this case, hydrostatic equilibrium of the thin H I layer is still a valid premise, provided that the value of the turbulent velocity dispersion is taken con-

⁴ Gravitational torques may be produced by a companion galaxy (e.g., Weinberg & Blitz 2006) or by cosmic infall accretion of protogalactic material in the outer halo (Ostriker & Binney 1989).

sistently. The scarce impact of massive high velocity clouds may break down hydrostatic equilibrium but only locally.

3.5.6 Uncertainties in the surface density of the outer disc

Our mass model does not include stellar streams as those detected recently (Newberg et al. 2002; Ibata et al. 2003; Yanny et al. 2003; Martin et al. 2005; Martínez-Delgado et al. 2005). Since a ring-like mass concentration produces an enhanced vertical acceleration in MOND, the presence of such structures are sufficient for explaining the relatively low flaring as compared to the predicted values at $R \sim 27$ kpc in Fig. 4. We refrain to find the best-fitting model until the distribution of the mass in the stellar disc is measured more accurately.

3.6 MOND versus CDM

One is tempted to ask: which competitive model, MOND or dark matter, reproduces the flaring of our Galaxy with the fewest ad-hoc assumptions? Narayan et al. (2005) and Kalberla et al. (2007) have explored the shape and density profile of the dark matter halo using the flaring technique. A nearly spherical dark halo as derived from Sgr dwarf constraints provides a very good fit to the observations as long as the dark matter density decays very fast, as r^{-4} (Narayan et al. 2005). In this situation, the total halo mass is $2.8 \times 10^{11} M_{\odot}$, too low to be acceptable. Accretion of homogeneous, diffuse intergalactic gas leads to more thin discs (Sánchez-Salcedo 2006), thereby going in the wrong direction to account for the observed flaring. A complex dark matter distribution (halo + disc + ring) as seen in Kalberla et al. (2007) may explain the thickness of the H I disc but it remains unclear if this model is compatible with the orbits of Sgr and its stellar debris. Kalberla et al. (2007) conclude that, if the dark matter particles only populates a rather spherical component with a flattening $0.9 \leq q \leq 1.25$ (Helmi 2004; Johnston et al. 2005; Law et al. 2005; Belokurov et al. 2006; Fellhauer et al. 2006), then the observed H I thickness is difficult to explain unless the effective velocity dispersion of the gas increases with galactocentric distance.

4 DISCUSSION AND CONCLUSIONS

Observations of spiral galaxies strongly support a one-to-one analytical relation between the inferred gravity of dark matter at any radius and the enclosed baryonic mass. This correlation of gravity with baryonic mass can be interpreted as a modification of gravity. If this is not the case, then the success of MOND is telling us something phenomenological about the nature of dark matter. Besides the shape of rotation curves of spirals, a wide range of gravitational effects appear in galactic dynamics, which in principle, offer independent restrictions on any proposed modified gravity scheme. Some examples include the dynamics of stars in the solar neighbourhood (Kuijken & Gilmore 1987), the ellipticity of the X-ray emission in elliptical galaxies (Buote & Canizares 1994), the gravitational stability of galactic discs (e.g., Sánchez-Salcedo & Hidalgo-Gómez 1999), the relaxation processes in stellar systems (Ciotti & Binney 2004;

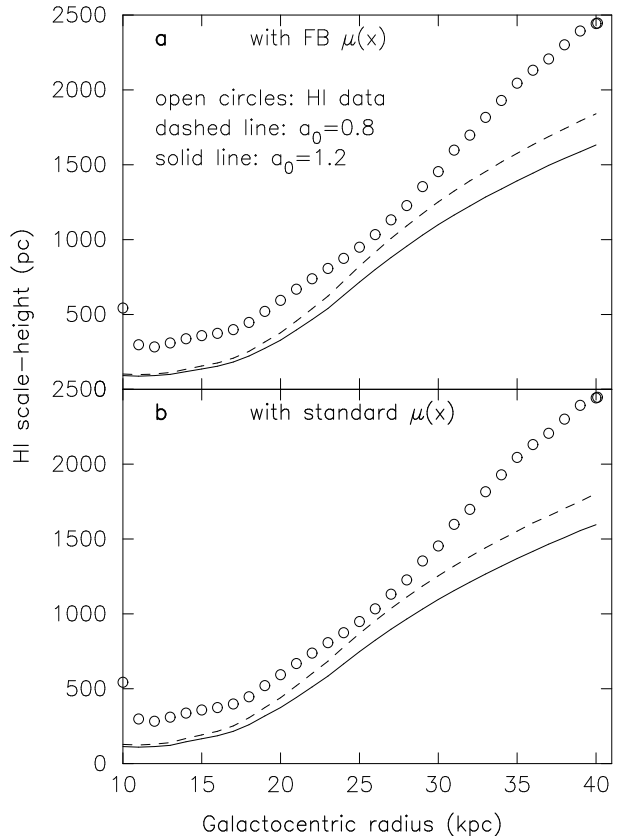


Figure 3. H I scaleheight vs R for the FB (upper panel) and the standard (lower panel) interpolating functions and $\sigma_{\text{HI}} = 7 \text{ km s}^{-1}$. The two curves are generated for two values of a_0 . Lower the value of a_0 better is the fit to the observed data. This is understandable since lower a_0 corresponds to lower values of v_c which means less gravitational pull. Beyond 27 kpc it really deviates from the observation for the above model parameters. a_0 is in units of $10^{-8} \text{ cm s}^{-2}$.

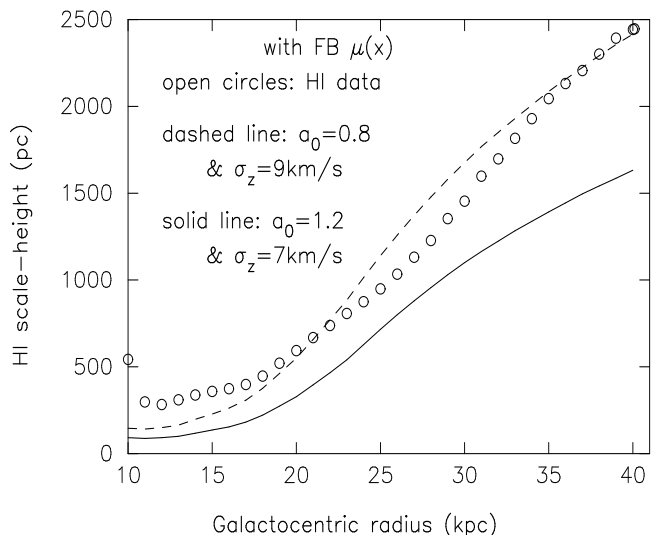


Figure 4. H I scaleheight vs R for the FB interpolating function with $a_0 = 0.8 \times 10^{-8} \text{ cm s}^{-2}$ and $\sigma = 9 \text{ km s}^{-1}$. For comparison, the scaleheight for $a_0 = 1.2 \times 10^{-8} \text{ cm s}^{-2}$ and $\sigma = 7 \text{ km s}^{-1}$ is also shown.

Sánchez-Salcedo et al. 2006) or the morphology of the Galactic warp (Weinberg & Blitz 2006). In this paper a new attempt to test the self-consistency of MOND has been carried out. Since in MOND all the gravity comes from the disc whereas the potential in CDM models is primarily from a spheroidal distribution, galactic discs are expected to be more flattened in MOND. For the same reason, if MOND is true, Newtonists should only infer oblate dark haloes. In this sense, a clear-cut inference of a prolate dark halo would be enough to rule out ‘classical’ MOND. Interestingly, studies on the shape and flattenings of dark haloes can be immediately used as tests to modified gravities.

Our knowledge about the shape of the Galactic dark halo is growing rapidly. Recent studies of the tidal debris from the Sagittarius dwarf and its bifurcation constrain the flattening of the dark halo potential to be close to spherical ($0.9 \leq q \leq 1.25$). Contrary to the naive expectation that MOND should produce far more precession because all gravity comes from the disc, Read & Moore (2005) found the amount of orbital precession is nearly identical to that which occurs in a CDM Galactic halo with $q = 0.9$.

The flaring of H I have also proven to be useful to constrain the flattening of dark haloes and is extremely sensitive to the dark matter distribution and to the law of gravity; MOND is expected to squeeze the disc into a thinner distribution because of the enhanced vertical acceleration. Kuijken & Gilmore (1989) test MOND in the context of the Oort discrepancy and find that it tends to overcorrect somewhat. However, they used a value of a_0 nearly 4 times larger than currently measured. Using the updated value for a_0 , McGaugh & de Blok (1998) and Famaey & Binney (2005) found the dynamics of stars to be consistent with MOND within the uncertainties. In this paper we first presented a framework to estimate the flaring of H I layers in MOND.

The MOND field equation is highly non-linear and much more complex than the classical Poisson field equation. Out of the plane it is not clear that the algebraic relation (Eq. 1) applies. In addition to the local self-gravity of the disc, MOND predicts a new term, the L -term, which has been shown to be equivalent to have a fictitious spherical dark matter halo. The self-gravity term and the L -term have very different radial dependences; the L -term is dominant beyond a certain critical radius. Both terms should work at phase to explain the observed flaring of galactic discs. If the L -term is ignored, the Galactic flaring is overestimated by a factor 5 at the last measured point $R = 40$ kpc.

Using this framework, an axisymmetric model was used to derive the mean H I flaring of the Milky Way predicted in MOND. Our Galaxy is particularly interesting because we have information about some parameters, such as the mass-to-light ratio, that are very difficult to obtain in other galaxies. It is by no means obvious that given the measured baryonic mass of the Milky Way with essentially no free parameters, MOND is able to explain the flaring of the H I disc in an extended radial range, between 10 and 40 kpc. Note, for instance, that so far the Galactic flaring is only understood in a dark matter scenario if the Galaxy contains a massive dark disc with a ring (Kalberla et al. 2007; de Boer et al. 2007).

In order to compare the observed gas-layer flaring to the predictions, the surface density of the baryonic components (stars and gas) and the gas velocity dispersion need to be

known. Since the baryonic distribution is well constrained from observations, the procedure is essentially with one free parameter σ_{HI} between 7 km s^{-1} and 9 km s^{-1} independent of radius. The results depend on the choice of the Galactic constants, since these values affect the gas distribution as inferred from observations. Following the IAU recommendations we take $R_\odot = 8.5 \text{ kpc}$ and $v_\odot = 220 \text{ km s}^{-1}$ and we have verified that, given the uncertainties, the results are robust to slight changes on the values of R_\odot and v_\odot .

For our reference set of parameters (local surface density of stars of $45 \text{ M}_\odot \text{ pc}^{-2}$ and $R_d = 3.2 \text{ kpc}$), we have found that MOND successfully reproduces the most recent and accurate flaring curve beyond $R = 17 \text{ kpc}$ for both standard and FB interpolating functions, provided the vertical velocity dispersion of H I is taken $\sim 9 \text{ km s}^{-1}$ as that observed in the inner Galaxy (Malhotra 1995; see also Blitz & Spergel 1991). In the interval $10 \text{ kpc} < R < 15 \text{ kpc}$, the observed scaleheight is 40% and 70% in excess of that predicted by MOND for the standard ($n = 2$) and the FB ($n = 1$) interpolating functions, respectively. Clearly, the reduced thickness predicted by MOND is unsatisfactory. We have verified whether uncertainties in the assumed parameters can ameliorate this discrepancy without altering the good fit at large radii ($R > 17 \text{ kpc}$). Interestingly, MOND fails at those radii where the dominant term in the field equation is not the confining force of the L -term but the local self-gravity component, thus $h \propto \mu \sigma^2 / \Sigma$. Therefore, a reduction on the adopted local stellar surface density or, equivalently, on Υ would result in a thicker H I disc in the region of interest. We have seen that by adopting the smallest Υ compatible with observations, h increases about 27% in the inner disc. On the other hand, the scaleheight also depends on the orbital acceleration v_c^2/R through μ . A reduction of the adopted value for R_\odot goes in the good direction to mitigate the overcorrection but the effect is rather irrelevant. For instance, if we assume $R_\odot = 8 \text{ kpc}$ instead of 8.5 kpc , h varies only $\sim 3\%$ at $10 \text{ kpc} < R < 15 \text{ kpc}$.

The simplest way to reconcile predictions with observations is to argue that ordered and small-scale magnetic fields and cosmic rays could contribute to support the disc within the optical disc ($R < 15 \text{ kpc}$). Depending on n and Υ , the effective velocity dispersion required to match observations should be a factor ~ 1.12 – 1.3 larger than the turbulent velocity dispersion. We have seen that, in principle, magnetic fields and cosmic rays could account for this. An enhanced effective velocity dispersion within the optical disc ($R < 15 \text{ kpc}$) is reasonable in a scenario where supernovae explosions feed up turbulence. An enhancement $\sigma'_{\text{HI}}/\sigma_{\text{HI}} = 1.3$ required to explain the flaring when $n = 1$ and a local stellar density of $\Sigma_\star = 45 \text{ M}_\odot \text{ pc}^{-2}$ is likely on the high side. Therefore, we can say that MOND satisfactorily explains the flaring provided that $n \geq 1$ and $\Sigma_\star < 45 \text{ M}_\odot \text{ pc}^{-2}$.

Very little further progress is likely to be made without further empirical constraints on the effects of non-thermal terms. If we learn in future that the non-thermal pressure forces from cosmic rays and magnetic fields have no role to play in the vertical support of H I discs (e.g., if the filling factor of H I is very low), then studies of the vertical distribution of cold gas in our Galaxy could either rule out MOND or, if MOND holds true, pose strong constraints on the stellar mass-to-light ratio of the Galactic disc and the form of the interpolating function. So far, this analysis is premature be-

cause we believe that a certain level of non-thermal support is more realistic.

The maps of H I surface density and scaleheight in our Galaxy are far from being axisymmetric. Nevertheless, the narrow anticorrelation between H I surface density and the thickness of the H I layer (see Figs. 1 and 4 in Levine et al. 2006b) is expected when the self-gravity of the gas is significant in negotiating the hydrostatic equilibrium, as occurs naturally in MOND. Given the present uncertainties in the vertical support by magnetic fields and cosmic rays, we conclude that MOND can plausibly explain the Galactic flaring and cannot be excluded as an alternative to dark matter. In order to discriminate between MOND and dark matter, we plan to extend the analysis for a sample of galaxies of different types, including dark dominated LSB and dwarf galaxies, with accurate determinations of the rotation curve and H I flaring.

Acknowledgements

We are grateful to Peter Kalberla for providing the tables of H I surface density and scaleheight from the LAB survey. We thank the anonymous referee for his/her critical reading of the manuscript and helpful comments that lead to an improvement of the paper. We also thank J. Cantó and F. Masset for interesting discussions.

REFERENCES

- Abramova, O. V., & Zasov, A. V. 2007, *Astronomy Reports*, in press (arXiv:0710.0257v1)
- Beck, R., Brandenburg, A., Moss, D., Shukurov, A., Sokoloff, D. 1996, *ARA&A*, 34, 155
- Beck, R. 2001, in Diehl R., Kallenbach R., eds, *The Astrophysics of Cosmic Rays*. Kluwer, Dordrecht
- Beck, R. 2007, *A&A*, 470, 539
- Becquaert, J.-F., Combes, F. 1997, *A&A*, 325, 41
- Begeman, K.G., Broeils, A.H., & Sanders, R.H. 1991, *MNRAS*, 249, 523
- Bekenstein, J. D. 2004, *Phys. Rev. D*, 70, 083509
- Bekenstein, J., & Milgrom, M. 1984, *ApJ*, 286, 7
- Belokurov, V., et al. 2006, *ApJ*, 642, L137
- Benjamin, R. A., & Danly, L. 1997, *ApJ*, 481, 764
- Bissantz, N., Englmaier, P. & Gerhard, O. 2003, *MNRAS*, 340, 949
- Blitz, L., & Spergel, D. N. 1991, *ApJ*, 370, 205
- de Boer, W., Gebauer, I., Weber, M., Sander, C., Zhukov, V., & Kazakov, D. 2007, arXiv:0710.5106
- Booth, C. M., & Theuns, T. 2007, *MNRAS*, 381, L89
- Bottema, R., Pestaa, J. L. G., Rothberg, B., & Sanders, R. H. 2002, *A&A*, 393, 453
- Boulares, A., & Cox, D. P. 1990, *ApJ*, 365, 544
- Brada, R., & Milgrom, M. 1995, *MNRAS*, 276, 453
- Buote, D. A., & Canizares, C. R. 1994, *ApJ*, 427, 86
- Ciotti, L. & Binney, J., 2004, *MNRAS*, 351, 285
- Clemens, D.P. 1985, *ApJ*, 295, 422
- Cuddeford, P. & Binney, J. 1993, *Nature*, 365, 20
- Dib, S., Bell, E., & Burkert, A. 2006, *ApJ*, 638, 797
- Diplas, A., & Savage, B. D. 1991, *ApJ*, 377, 126
- Elmegreen, B. G., & Hunter, D. A. 2000, *ApJ*, 540, 814
- Famaey, B., & Binney, J. 2005, *MNRAS*, 363, 603
- Famaey, B., Gentile, F., Bruneton, J.-P., & Zhao, H.S. *Phys. Rev. D*, 75, 063002
- Fellhauer, M., et al. 2006, *ApJ*, 651, 167
- Fletcher, A. & Shukurov, A. 2001, *MNRAS*, 325, 312
- Flynn, C., & Fuchs, B. 1994, *MNRAS*, 270, 471
- Flynn, C., Holmberg, J., Portinari, L., Fuchs, B., & Jahreiß, H. 2006, *MNRAS*, 372, 1149
- Gómez, G. C., & Cox, D. P. 2002, *ApJ*, 580, 235
- Gómez, G. C., & Cox, D. P. 2004, *ApJ*, 615, 744
- Helmi, A. 2004, *ApJ*, 610, L97
- Hernquist, L., & Quinn, P. J. 1987, *ApJ*, 312, 17
- Holmberg, J. & Flynn, C. 2004, *MNRAS*, 352, 440
- Honma, M. & Sofue, Y. 1997, *PASJ*, 49, 453
- Ibata, R. A. et al., 2003, *MNRAS*, 340, L21
- Jenkins, A., & Binney, J. 1990, *MNRAS*, 245, 305
- Johnston, K. V., Law, D. R., Majewski, S. R. 2005, *ApJ*, 619, 800
- Kalberla, P. M. W. 2003, *ApJ*, 588, 805
- Kalberla, P.M.W., & Kerp, J. 1998, *A&A*, 339, 745
- Kalberla, P. M. W., Burton, W. B., Hartmann, D., Arnal, E. M., Bajaja, E., Morras, R., & Pöppel, W. G. L. 2005, *A&A*, 440, 775
- Kalberla, P. M. W., Dedes, L., Kerp, J., & Haud, U. 2007, *A&A*, 469, 511
- Kerr, F. J., & Lynden-Bell, D. 1986, *MNRAS*, 221, 1023
- Kuijken, K., & Gilmore, G. 1989, *MNRAS*, 239, 605
- Larsen, J. A., & Humphreys, R. M. 2003, *AJ*, 125, 1958
- Law, D. R., Johnston, K. V., & Majewski, S. 2005, *ApJ*, 619, 807
- Levine, E. S., Blitz, L. & Heiles, C. 2006a, *ApJ*, 643, 881
- Levine, E. S., Blitz, L. & Heiles, C. 2006b, *Science*, 312, 1773
- Lewis, J.R. & Freeman, K.C. 1989, *AJ*, 97, 139
- López-Corredoira, M., Cabrera-Lavers, A., Garzón, F., & Hammersley, P. L. 2002, *A&A*, 394, 883
- Malhotra, S. 1995, *ApJ*, 448, 138
- Martin, N. F., Ibata, R. A., Conn, B. C., Lewis, G. F., Bellazzini, M., & Irwin, M. J. 2005, *MNRAS*, 362, 906
- Martínez-Delgado, D. et al., 2005, *ApJ*, 633, 205
- Masset, F. 1997, PhD thesis, University of Paris 7
- McGaugh, S. S. 2004, *ApJ*, 609, 652
- McGaugh, S. S. 2005, *Phys. Rev. Lett.*, 95, 171302
- McGaugh, S. S., & de Blok, W. J. G., 1998, *ApJ*, 499, 66
- Mera, D., Chabrier, G., & Schaeffer, R. 1998, *A&A*, 330, 953
- Merrifield M. R. 2002, in Natarajan P., ed., *The Shapes of Galaxies and Their Dark Matter Halos*, Singapore, World Scientific, 170
- Milgrom, M. 1983, *ApJ*, 270, 365
- Milgrom, M. 1986, *ApJ*, 306, 9
- Milgrom, M. 1995, *ApJ*, 455, 439
- Milgrom, M. 2001, *MNRAS*, 326, 1261
- Narayan, C.A. & Jog, C. J. 2002, *A&A*, 394, 89
- Narayan, C. A., Saha, K., & Jog, C. J. 2005, *A&A*, 440, 523
- Newberg, H.J., et al., 2002, *ApJ*, 569, 245
- Nipoti, C., Londrillo, P., Zhao, H. S., & Ciotti, L. 2007, *MNRAS*, 379, 597
- Olling, R. P. 1995, *AJ*, 110, 591
- Olling, R. P. 1996, *AJ*, 112, 481
- Olling, R. P., & Merrifield, M. R. 2000, *MNRAS*, 311, 361
- Olling, R. P., & Merrifield, M. R. 2001, *MNRAS*, 326, 164
- Ostriker, E. C., & Binney, J. J. 1989, *MNRAS*, 237, 785
- Parker, E. N. 1966, *ApJ*, 145, 811
- Petric, A. O., & Rupen, M. P. 2007, *AJ*, 134, 1952
- Read, J. I., & Moore, B. 2005, *MNRAS*, 361, 971
- Reid, M. J., Readhead, A. C. S., Vermeulen, R. C., & Treuhaft, R. N. 1999, *ApJ*, 524, 816
- Sánchez-Salcedo, F. J. 2004, *J. Korean Astron. Soc.*, 37, 205
- Sánchez-Salcedo, F. J. 2006, *MNRAS*, 365, 555
- Sánchez-Salcedo, F. J. & Hidalgo-Gómez, A. M. 1999, *A&A*, 345, 36
- Sánchez-Salcedo, F. J., & Lora, V. 2005, in Val Blain J., ed., *Progress in Dark Matter Research*, Nova Science Publishers, Inc., 73
- Sánchez-Salcedo, F. J., & Reyes-Ruiz, M. 2004, *ApJ*, 607, 247

- Sánchez-Salcedo, F. J., Reyes-Iturbide, J., & Hernandez, X. 2006, MNRAS, 370, 1829
- Sanders, R. H. 1996, ApJ, 473, 117
- Sanders, R. H., & McGaugh, S. S. 2002, ARA&A, 40, 263
- Sanders, R. H., & Noordermeer, E. 2007, MNRAS, 379, 702
- Sanders, R.H. & Verheijen, M.A.W. 1998, ApJ, 503, 97
- Santillán, A., Sánchez-Salcedo, F. J., & Franco, J. 2007, ApJ, 662, L19
- Sellwood, J. A., & Balbus, S. A. 1999, ApJ, 511, 660
- Sommer-Larsen, J., Götz, M., & Portinari, L. 2003, ApJ, 596, 47
- Spitzer, L. 1978, Physical Processes in the Interstellar Medium. John Wiley & Sons, New York
- Stubbs, C.W., & Garg, A. 2005, astro-ph/0512067
- Weinberg, M. D., & Blitz, L. 2006, ApJ, 641, L33
- Wouterloot, J.G.A., Brand, J., Burton, W.B., & Kwee, K.K. 1990, A&A, 230, 21
- Yanny, B. et al., 2003, ApJ, 588, 824
- Zweibel, E. G., & McKee, C. F. 1995, ApJ, 439, 779

APPENDIX A: ESTIMATING THE MAGNITUDES OF ξ_Φ AND ξ_μ

In an isothermal self-gravitating disc with one dimensional dispersion σ , the vertical acceleration at a scaleheight h is $1.5\sigma^2/h$ and the radial acceleration is v_c^2/R . Thus the ratio between the vertical and radial accelerations is $\xi_\Phi = 1.5(\sigma/v_c)^2(R/h)$. In our Galaxy, ξ_Φ can be computed for the H I layer to be 0.14 and 0.05 at 15 and 40 kpc, respectively. At regions where $\xi_\Phi \ll 1$, i.e. $h > 1.5(\sigma/v_c)^2 R$, the radial component determines the kinematics of the disc. For a galaxy like the Milky Way, this occurs at $R > 6$ kpc for the stellar disc and at $R \gtrsim 1$ kpc for the H I disc. At these radii, we have

$$|g_z| \simeq \frac{2\pi G \Sigma(z)}{\mu(x)}, \quad (\text{A1})$$

and

$$|g_R| \simeq \frac{v_c^2}{R}, \quad (\text{A2})$$

with

$$x(R, z) = \frac{|\vec{\nabla}\Phi|}{a_0} \simeq \frac{|g_R|}{a_0} = \frac{v_c^2}{Ra_0} \quad (\text{A3})$$

where $\Sigma(z) \equiv \int_{-z}^z \rho(z') dz'$ is the surface density within a slab of thickness $2z$, and $v_c^2(R, z) \equiv R(\partial\Phi/\partial R)$ is the squared planar circular velocity.

In order to evaluate ξ_μ , we need to estimate $\partial g/\partial z$ at $z \simeq h$. It is simple to show that

$$\left. \frac{\partial g}{\partial z} \right|_{z=h} \simeq 2g_z \left. \frac{\partial g_z}{\partial z} \right|_{z=h} \simeq \frac{\pi^2 G^2 \Sigma_\infty^2}{\mu^2 h} = 4 \frac{\sigma^4}{h^3}, \quad (\text{A4})$$

where we have used Eq. (A1) and the relation $\sigma^2 \approx \pi\mu^{-1}G\Sigma_\infty h$. On the other hand

$$\left. \frac{\partial g}{\partial R} \right|_{z=h} \simeq -2 \frac{v_c^4}{R^3}. \quad (\text{A5})$$

Combining the above equations, we obtain:

$$|\xi(R)| \approx 3 \left(\frac{R}{h} \right)^4 \left(\frac{\sigma}{v_c} \right)^6. \quad (\text{A6})$$

For illustration, we may compute ξ for the Milky Way at $R = 15$ kpc and $R = 40$ kpc. At $R = 15$ kpc, $\xi \approx 0.15$ and decreases to $\xi \approx 0.0016$ at 40 kpc.